Journal of Membrane Science and Research 3 (2017) 296-302

Journal of Membrane Science & Research

journal homepage: www.msrjournal.com

Research Paper

Kinetic Modelling of Hydraulic Resistance in Colloidal System Ultrafiltration: Effect of Physiochemical and Hydrodynamic Parameters

Seyed M.A. Razavi*, Ali Alghooneh, Fataneh Behrouzian

Division of Food Engineering, Department of Food Science and Technology, Ferdowsi University of Mashhad (FUM), POBox: 91775-1163, Mashhad, Iran

Article info

Received 2016-08-15
Revised 2017-04-06
Accepted 2017-04-10
Available online 2017-04-10

Keywords

Colloid
Dynamic modeling
Kinetic
Resistance
Skim milk
Ultrafiltration

Highlights

- We developed three semi-empirical models on dynamic resistance modeling.
- Resistances altered by transmembrane pressures, pH, salt, flow rate and temperature.
- Extent, rate of rise, initial and semi-steady resistances, termed by kinetic model.
- Increasing applied variables enhanced the kinetic model terms except the flow rate.
- Transmembrane pressure was the main factor on the rate of resistance growth.

Graphical abstract

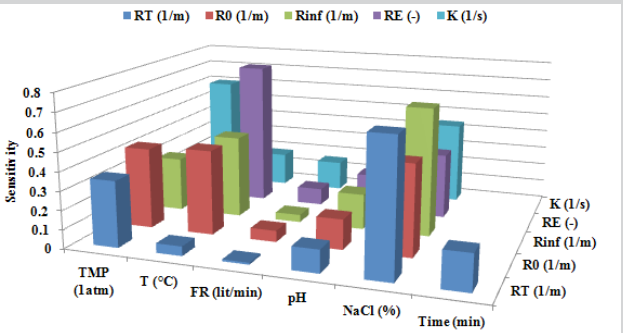

Sensitivity analyses of the input parameters for prediction of dynamic hydraulic resistance and kinetic model parameters (R_0, initial hydraulic resistance; R_∞, infinite (steady-state) hydraulic resistance; R_E, resistance increment extent and k resistance increment rate) in crossflow ultrafiltration of skimmilk.

Abstract

In this work, different kinetic patterns (homographic, exponential-linear and exponential) of hydraulic resistance in ultrafiltration process of a colloidal system have been investigated. Exponential kinetic model, as the best approach, was employed for description of dynamic hydraulic resistance of skim milk ultrafiltration at different feed flow rates (FR) (10, 30 and 46 L/min), transmembrane pressures (TMP) (0.3, 0.6 and 1 atm), temperatures (30, 40 and 50°C), pH levels (5.6, 6, 6.6, 6.9 and 7.6) and NaCl concentrations (0, 0.03, 0.06 and 0.12 %w/w). Results indicated that the initial resistance (R_0), steady-state resistance (R_∞), resistance increment rate (k) and resistance increment extent (R_E) increased with TMP and ionic strength increasing and FR decreasing. The most sensitive factor for prediction of R_T (total hydraulic resistance), R_0 and R_∞ was the NaCl concentration. Also, the highest sensitive factors for R_E and k were temperature (0.77) and TMP (0.60), respectively.

1. Introduction

By applying UF membrane technology to the milk processing, milk can be modified by separating, clarifying, or fractionating a selected component in milk from other components [1]. Milk is a complex system and has diverse components which make the membrane separation practicable but dependent on hydrodynamic and physicochemical operating conditions of the UF process [2, 3]. However, both fouling and concentration polarization limited the widespread application of membrane separation in dairy processing industry [4, 5]. The difficulty of fouling analyzing is that many phenomena occurring simultaneously on the membrane surface [6] and it is not very clear how the hydrodynamic and physicochemical operating conditions affect fouling processes in crossflow filtration.

As the membrane resistances are affected by the primary factors of the

* Corresponding author at: Phone: +98 51 3880 5763; fax: +98 51 38763842
E-mail address: s.razavi@um.ac.ir (S.M.A. Razavi)

DOI: 10.22079/JMSR.2017.47339.1097

temperature, we studied the effect of a wide range of these parameters on the total hydraulic resistance kinetic pattern of skim milk system [7, 8]. There are some hydraulic resistance models which explain the governing mechanisms of filtration, some of them are simple, while other ones are complex and difficult to fit to experimental data. The problem is that these models generally consider just one mechanism for the whole filtration process [9]. As, there is not a completely theoretical model to quantitatively describe hydraulic resistance kinetic pattern involved in ultrafiltration processes very accurately, there is a need for alternative such as empirical models.

Several empirical models have been found in the literature to analyze the fouling of UF [10-13]. Preferentially, a desirable mathematical representation of a physical phenomenon should include characteristics such as: (*i*) the least number of constants, (*ii*) the constants and the equation components which transmit meaningful physical information, (*iii*) the equation is sensitive to variable physical parameters in the system; and (*iv*) the mathematical structure of the equation is uncomplicated. Some of these models are investigated in this study. These models are able to determine the initial resistance, steady-state resistance, resistance increment rate and resistance increment extent, so could help us to realize the kinetic pattern of all hindering factors growth (resistance offered by the membrane and by the irreversible and reversible fouling) in a wide range of hydrodynamic and physicochemical operating conditions in ultrafiltration of colloidal systems like skim milk. To the best of our knowledge, the mentioned models have not yet been used in any membrane experiments for the description of membrane ultrafiltration hydraulic resistance kinetic pattern. Therefore, the objectives of this study were (*i*) to evaluate the effect of different conditions such as pH, NaCl content, transmembrane pressure (TMP), temperature, and feed flow rate (FR) on total hydraulic resistance (R_T) during milk ultrafiltration as a case study; and (*ii*) to model dynamically the hydraulic resistance-time profile with a view to obtain a deep understanding of the phenomena involved in the performance of the crossflow ultrafiltration system.

2. Theory

Generally, the physics of hydraulic resistance models are evaluated using the series resistance equation based on the electric–hydraulic analogy. In this work, based on the characteristic shape of hydraulic resistance-time profile of colloidal ultrafiltration systems, we concerned with this phenomena regarding its rate of change, extent of change, change pattern during time and parameters such as initial and steady state hydraulic resistances using three kinetic models, i.e., homographic, exponential-linear and exponential models. These mathematical models are used in this work to describe the dynamic hydraulic resistance of a vast set of experimental data.

2.1. Homographic kinetic model

Investigation of total hydraulic resistance-time curves feature showed that there was similarity to some physical phenomena such as battery charging [14], water absorption [15] and creep behaviour of materials [16]. Herein, we used this procedure for interpretation of total hydraulic resistance-time curve. First, we normalized the experimental hydraulic resistance-time data using the following relationship:

$$Y(t) = \frac{(R(t) - R_0)}{R_m} \tag{1}$$

where $R(t)$ is the hydraulic resistance after time t, R_0 is the initial hydraulic resistance, and R_m is intrinsic resistance of the membrane. As the linear form can simplify verification of the goodness of the equation and calculation of its constants; the normalized curve was linearized by Eq. (2):

$$\frac{t}{Y(t)} = k_1 + (k_2 \times t) \tag{2}$$

where $1/k_1$ and $1/k_2$ represent the initial growth rate of hydraulic resistance and asymptotic level of $Y(t)$, when $t \to \infty$, respectively. Based on Eq. (2), the steady-state hydraulic resistance was given as follows:

$$R_\infty = (R_m \times \frac{1}{k_2}) + R_0 \tag{3}$$

2.2. Exponential-linear kinetic model

In the mentioned model, it was assumed that the total hydraulic resistance growth has three distinct stages: First, a time-independent stage; second, an exponential time-dependent stage and third, a linear time-dependent stage. Afterward, the appropriate model was chosen to describe all of these stages as follows:

$$R(t) = R_0 + [R_1 \times \left(1 - exp\left(-\frac{t}{\lambda}\right)\right)] + (R_2 \times t) \tag{4}$$

where R_0 is the initial hydraulic resistance, R_1 and R_2 are the hydraulic resistances of the nonlinear and linear part of curve, and $1/\lambda$ is the initial growth rate of hydraulic resistance. Also, according to this model, the steady-state hydraulic resistance was given as follows:

$$R_\infty = R_0 + R_1 \tag{5}$$

2.3. Exponential kinetic model

For investigating the relation of reaction rate and concentration of substrate in kinetic science, the following equation is used:

$$\frac{dc}{dt} = k \times (c_\infty - c)^n \tag{6}$$

Herein, to model the kinetics of hydraulic resistance in terms of initial resistance, steady-state resistance and the rate of resistance growth, the Eq. (6) is rewrite to the following differential equation form in order to relate the hindrance factor with time:

$$\frac{d\psi}{dt} = k \times (\psi_\infty - \psi)^n \tag{7}$$

where ψ_∞ is the hindering factor of the membrane when $t \to \infty$, k is the growth rate constant of hindering factor and n is the kinetic order of resistance change with time. For simplicity, the first kinetic order was assumed (n=1), so the Eq. (7) can be solved using the boundary conditions at time=0, $\psi(t) = \psi_0$ and at time= t, $\psi(t) = \psi_t$ as follows:

$$\ln \frac{(\psi_t - \psi_\infty)}{(\psi_0 - \psi_\infty)} = k \times t \tag{8}$$

In order to apply Eq. (8) to experimental hydraulic resistance-time data, we need to specify a relationship between ψ and hydraulic resistance, therefore, a dimensionless parameter of $\psi(t)$ was introduced as follows:

$$\psi(t) = \frac{(R_t - R_0)}{(R_\infty - R_0)} \tag{9}$$

Substituting Eq. (9) into Eq. (8) and the rearrangement of Eq. (8) yields:

$$R(t) = (R_0 - R_\infty) \times exp(-k \times t) + R_\infty \tag{10}$$

where, R_0, R_∞ and k are the initial hydraulic resistance, the infinite (steady-state) resistance and the resistance increment rate, respectively. The extent of resistance increment can be defined as follows:

$$R_E = \frac{(R_\infty - R_0)}{R_\infty} \tag{11}$$

3. Experimental

3.1. Material and membrane

Reconstituted skim milk was prepared by addition of medium heat skim milk powder (SMP) to warm distilled water (~50 °C) under fast stirring condition and employed as the feed for all experiments. The same batch of SMP was used in all experimental runs to make sure that change in measured parameters did not result from differences in milk composition. The composition of SMP is presented in Table 1. Twelve kilograms of reconstituted skim milk was used for each run. The polymeric hollow fibre membrane was supplied by Koch Membrane Systems, USA, composed of polyethersulfone, MWCO 10 kDa, providing effective area of 2.42 m^2 with capability of operating up to 1.2 atm pressure.

Table 1
Average chemical composition of skim milk samples [a]

Component	Average (%)	Range [b]
Protein	2.86	0.14
Fat	0.09	0.01
Lactose	4.73	0.28
Ash	0.77	0.05
Total solids	8.44	0.52
pH	6.54	0.01

[a] Each point is the mean of three replicates.
[b] Range means the difference between maximum and minimum value of each component.

3.2. Filtration setup

A schematic diagram of the pilot-scale ultrafiltration unit operated in this study is illustrated in Figure 1. The inlet and the outlet feed pressures were monitored by two pressure gauges which positioned as close to the inlet and the outlet of the membrane module as physically possible. The crossflow velocity was controlled by changing the rotation speed of the pump 2. The temperature of feed was continuously controlled by tubular heat exchanger and then monitored by a temperature probe attached to the feed tank during each run. The permeate flux was measured and recorded every 60 s.

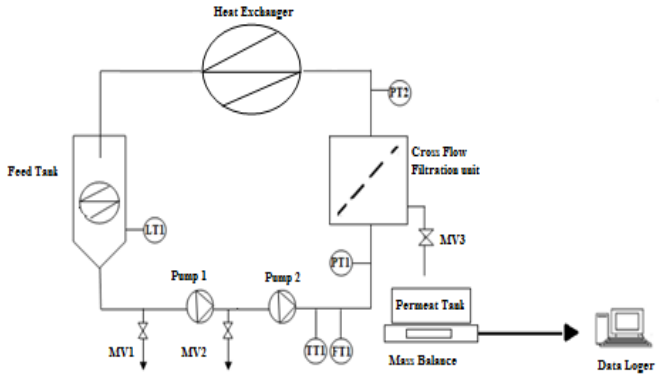

Fig. 1. Schematic diagram of ultrafiltration pilot plant system used in this study.

3.3. Filtration experiment

The effect of varying TMP (0.3, 0.6 and 1 atm), temperature (30 °C, 40 °C and 50 °C), flow rate (10, 30 and 46 L/min), pH of feed (5.6, 6.0, 6.6, 6.9 and 7.6) and the NaCl concentration (0, 0.03, 0.06 and 0.12 %w/w) on the total hydraulic resistance, were studied. The transmembrane pressure was calculated according to the following equation:

$$TMP = \frac{(P_i + P_0)}{2} - P_p \quad (12)$$

where P_i, P_o and P_p are inlet, outlet and permeate pressures, respectively.

The permeate flux dynamic was investigated over a period of 130 min. For each experimental run, the feed tank was first recycled with distilled water at the specified operating condition to warm up the system and to measure the intrinsic membrane resistance. We used the dependence of permeate flux (J_p) on transmembrane pressure (TMP) based on Darcy's law (Eq. (13)), allowing for hydraulic resistance encountered by the liquid flowing through the membrane:

$$R_T = \frac{TMP}{(\mu_p \times J_p)} \quad (13)$$

where μ_p is the permeate viscosity and R_T is the total hydraulic resistance.

The total hydraulic resistance is the sum of several resistances, e.g., the intrinsic membrane resistance and the reversible and irreversible fouling resistances. After the skim milk ultrafiltration processes, the leftover milk was removed from the system using water rinsing at 50 °C. After the rinsing procedure, cleaning was performed using 0.5% w/v Ultrasil11 at 50 °C for 20 minutes. The Ultrasil11 pH value was 12.9. After cleaning, the membrane was rinsed several times using water at 50 °C. For controlling the cleaning procedure, the water flux measurement was done at the start and end of each run, the difference between the two measured data checked to be less than 3-5 %, if not fouling was not removed and the cleaning method was repeated until the flux returned or the membrane was replaced with a new one. The kinematic viscosity and density of permeate samples were measured using an Ostwald U-tube capillary viscometer and a 25 ml picnometer, respectively.

3.4. Data analysis

Fitting and goodness of fit (R^2, coefficients of determination; R^2_{Adj}, adjusted R-squared and RMSE, root mean square error) were achieved by MATLAB 2010 (7.10.0), using the curve fitting toolbox and Trust-Region algorithm. The choice of the most appropriate model was based on the highest R^2 and R^2_{Adj} and the lowest RMSE values, which calculated by Eq. (14), Eq. (15) and Eq. (16), respectively:

$$R^2 = 1 - \frac{SS_{residual}}{SS_{residual} + SS_{model}} \quad (14)$$

$$R^2_{Adj} = 1 - \frac{\frac{SS_{residual}}{DF_{residual}}}{(\frac{SS_{residual}}{DF_{residual}} + \frac{SS_{model}}{DF_{model}})} \quad (15)$$

$$RMSE = \sqrt{\frac{\sum_{i=1}^{N}(O_i - T_i)^2}{N}} \quad (16)$$

where SS is the sum of squares, O_i is the i^{th} actual value, T_i is the i^{th} predicted value, N is the number of data and DF is the degree of freedom. In addition, for validation of models it is required a residual analysis in order to verify that residuals associated with the correlation has a normal distribution. In this case, Shapiro-Wilk (α=0.05) test was used. A sensitivity analysis was conducted to provide a measure of the relative importance among the inputs of the model and to illustrate how the model output varied in response to variation of an input.

4. Result and discussion

4.1. Model selection

The hydraulic resistance-time profile of skim milk ultrafiltration displayed a typical asymptotic behavior at all tests. Every model in this survey were directly applied to the experimental resistance–time data in various operating and physicochemical conditions to investigate which model can better describe the dynamic hydraulic resistance pattern. It was found that the exponential kinetic model best fitted the total hydraulic resistance versus time data (see Figure 2). In comparison, the fitness of exponential kinetic model was noticeably better than those can be achieved with theoretical and some other empirical models [11-13, 17-19]. Rajca et al. [18] found that relaxation model (a mathematical model based on the analysis of membrane hydraulic resistance and the mass transport balance during membrane filtration) did not fit adequately the initial part of the resistance-time curve of raw water reservoir UF process. The experimental data and the results of fitting using exponential kinetic model to simulate total resistance-time pattern during milk ultrafiltration at various temperature, TMP, flow rate, pH and ionic strength are demonstrated in Figures 3-7, respectively. As it is seen, the exponential kinetic model predicted well the complex behavior (non-linearity) of resistance-time profile at different conditions. There was excellent agreement between the experimental data and predictions at all cases, (R^2>0.90, R^2_{adj}>0.91 and RMSE<0.03). Furthermore, the residual analysis verified that residuals associated with the correlation of this model have normal distribution which showed the acceptable predictability of exponential kinetic model. Besides its outstanding ability to describe the experimental resistance-time data, the model parameters were of highly practical significance in determining the initial resistance (R_0), steady state resistances (R_∞), rate of resistance increment (k) and the extent of resistance increment (R_E) in all the tested conditions, which would be discussed in the following sections. Using these parameters, it is possible to predict hydraulic resistance at any time under a given operating condition.

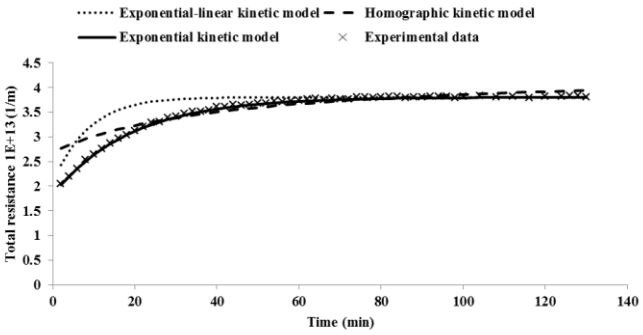

Fig. 2. Fitting ability of three semi-empirical models to experimental data of total hydraulic resistance -time profile (NaCl concentration 0.12%, Temperature 50°C, TMP 1.0 atm, pH= 6.6 and flow rate 56 L/min).

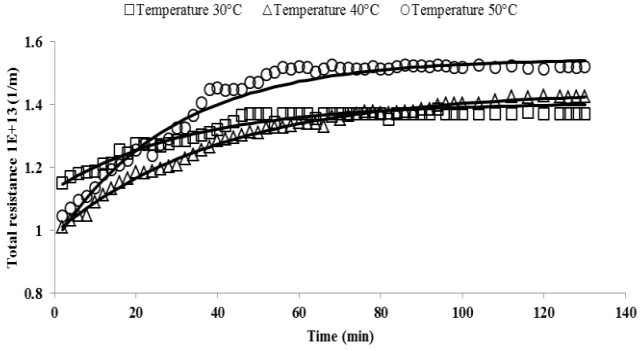

Fig. 3. Dynamic hydraulic resistance predictions during the skim milk ultrafiltration as a function of temperature (TMP 1 atm, pH= 6.6, flow rate 12 L/min, 0%NaCl and –, exponential kinetic model predictions).

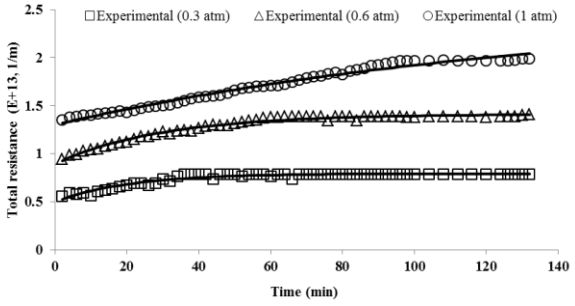

Fig. 4. Dynamic hydraulic resistance predictions during the skim milk ultrafiltration as a function of transmembrane pressure (temperature 40 °C, pH= 6.6, flow rate 30 L/min and 0%NaCl –, exponential kinetic model predictions).

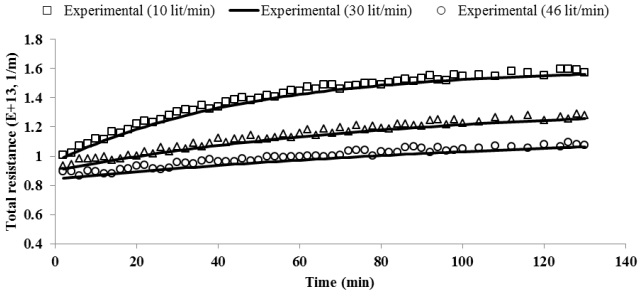

Fig. 5. Dynamic hydraulic resistance predictions during the skim milk ultrafiltration as a function of crossflow velocity (Temperature 50°C, TMP 0.3 atm, pH= 6.6, 0%NaCl and –, exponential kinetic model predictions).

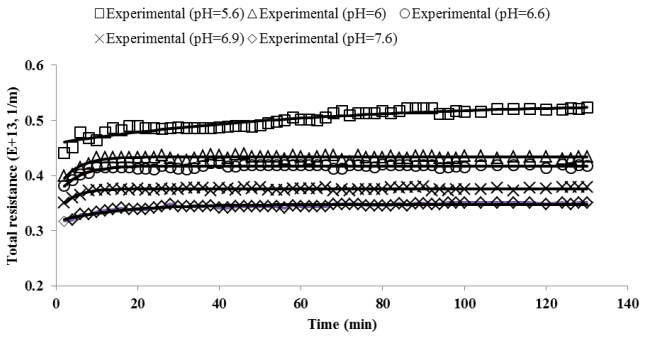

Fig. 6. Dynamic hydraulic resistance predictions during the skim milk ultrafiltration as a function of pH (Temperature 30°C, TMP 0.3 atm, flow rate 15 L/min, 0%NaCl and –, exponential kinetic model predictions).

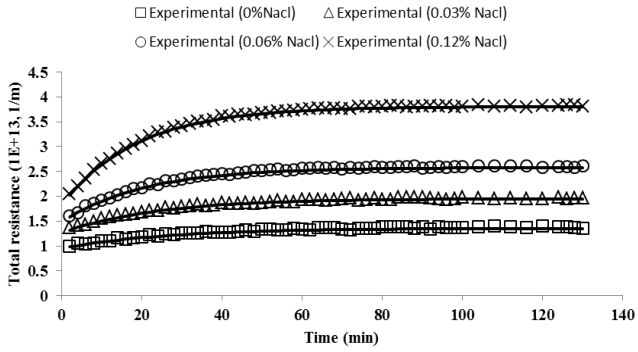

Fig. 7. Dynamic hydraulic resistance predictions during the skim milk ultrafiltration as a function of NaCl concentrations (Temperature 50°C, TMP 1.0 atm, pH= 6.6, flow rate 56 L/min and –, exponential kinetic model predictions).

4.2. Effect of temperature

The results of modeling for dynamic hydraulic resistance at three temperatures (30, 40, and 50 °C) are demonstrated in Table 2. R_0, R_∞, R_E *and* k parameters varied significantly with temperature. According to Table 2, R_0 decreased with the elevation of temperature, which may be because, the viscosity of the bulk fluid decreased and the molecules' motion increased at higher temperature, thereby, the diffusion constant of skim milk components increased and the effect of concentration polarization diminished. [20]. Furthermore, an increase in temperature can expand the pore radius of membrane [7]. As time passed, other resistance parameters (R_∞, R_E *and* k) increased with temperature (see Table 2). The effect of each 1 °C increase of temperature on R_E and all the kinetic model parameters at the range of 30 to 40 °C were almost twice of those at 40 to 50 °C. In addition, the most sensitive parameter to temperature was k at both temperature ranges (see Table 3). At low temperature, molecules of skim milk have low activation energy, so, these molecules adsorb on the membrane surface with weak bonds such as the hydrogen bonds. However, at higher temperature, chemical reactions influence the interaction between solutes and membrane [7,20], which results in the increase of steady-state resistance, resistance increment rate and resistance increment extent values (see Table 2). Moreover, the enhancement of solutes diffusion can lead to higher accessibility of foulants into the pores, thus increases the membrane pore blocking fouling [21]. In addition, the increment of the temperature increases slightly the osmotic pressure [22]. Razavi et al. [12] found that the total hydraulic resistance increased with temperature during ultrafiltration of skim milk. In other words, temperature has a bilateral effect on total resistance.

4.3. Effect of transmembrane pressure

The results of fitting hydraulic resistance-time data with exponential kinetic model at various TMPs (temperature 40 °C, pH= 6.6, flow rate 30 L/min and 0%NaCl) are presented in Table 2. Results showed that there was weak form of critical flux in all experiments. For the weak form of critical flux, it is assumed that there is very rapid fouling on start-up which consists of both intrinsic membrane resistance and concentration polarization and so the flux-TMP relationship is below that of the pure water line. The critical flux is the point at which this line becomes non-linear [23]. The critical

pressure and flux were determined according to Astudillo-Castro method [21], which were equal to 0.451 atm and 0.381 kg/m^2.min, respectively, indicating that up to 0.451 atm, flux reduction was induced by concentration polarization (reversible resistance), and fouling (irreversible resistance) was not exist in this region. This region is ideal for membrane process. The TMP higher than critical pressure resulted in fouling phenomena. In addition, the limiting flux (Eq. 17) and limiting pressure (Eq. 18) were determined as follows [24]:

$$J_C = 0.632 \times J_{lim} \quad (17)$$

$$(\Delta P_T)_L = -(\Delta P_T)_C \times \ln(1 - 0.95) \approx 3(\Delta P_T)_C \quad (18)$$

The limiting flux and pressure were 0.631 kg/m^2.min and 1.353 atm, respectively, while the maximum of pressure in all experimental runs was 1 atm. So, any of the experimental runs was not in the limiting flux region.

The R_0, R_∞, R_E *and* k parameters increased significantly as TMP increased (see Table 2). Each 0.1 atm enhancement in the TMP at the range of 0.3-0.6 atm and 0.6-1.0 atm resulted in an increase in R_E by 4.21 and 2.78%, and k parameter by 3.81 and 6.21%, respectively, indicated higher sensitivity of R_E to the lower TMP range and k to the higher TMP range (see Table 3). On the other hand, the effect of each 0.1 atm enhancement in the TMP on the increase of R_0 and R_∞ did not show significant differences between two mentioned TMP ranges. In addition, 0.1 atm increase in TMP showed higher impact on k and R_E than R_0 and R_∞. This phenomenon may have several reasons. For example, with increase in TMP, the deposit progressively spreads and reaches the opening of the membrane channel.

Table 2
Parameters of exponential kinetic model determined for the total hydraulic resistance-time profile at different operating and physio-chemical conditions of skim milk ultrafiltration*

Conditions						exponential kinetic model parameters			
Variable	**Temperature (°C)**	**TMP (atm)**	**Flow rate (L/min)**	**pH**	**NaCl (%)**	**R_0 ($\times 10^{13}$)**	**R_∞ ($\times 10^{13}$)**	**R_E**	**K (1/s)**
Temperature	*30*	1.0	12	6.6	0.0	1.131^{b} ± 0.030	1.405^{a} ± 0.039	0.195^{a} ± 0.005	0.021^{a} ± 0.001
	40	1.0	12	6.6	0.0	1.074^{b} ± 0.040	1.484^{b} ± 0.007	0.277^{b} ± 0.007	0.029^{a} ± 0.003
	50	1.0	12	6.6	0.0	0.998^{a} ± 0.031	1.546^{c} ± 0.006	0.354^{c} ± 0.009	0.047^{b} ± 0.004
TMP	40	*0.3*	30	6.6	0.0	0.641^{a} ± 0.071	0.903^{a} ± 0.090	0.290^{a} ± 0.021	0.007^{a} ± 0.002
	40	*0.6*	30	6.6	0.0	0.792^{b} ± 0.055	1.217^{b} ± 0.126	0.349^{b} ± 0.016	0.016^{b} ± 0.004
	40	*1.0*	30	6.6	0.0	0.890^{b} ± 0.072	1.463^{c} ± 0.101	0.391^{c} ± 0.019	0.028^{c} ± 0.006
Flow rate	50	0.3	*10*	6.6	0.0	0.962^{b} ± 0.062	1.598^{b} ± 0.090	0.398^{b} ± 0.028	0.021^{b} ± 0.003
	50	0.3	*30*	6.6	0.0	0.902^{ab} ± 0.051	1.351^{ab} ± 0.178	0.332^{a} ± 0.030	0.012^{a} ± 0.002
	50	0.3	*46*	6.6	0.0	0.843^{a} ± 0.058	1.185^{a} ± 0.113	0.288^{a} ± 0.037	0.008^{a} ± 0.002
pH	30	0.3	15	*5.6*	0.0	0.458^{b} ± 0.048	0.534^{e} ± 0.008	0.143^{d} ± 0.004	0.015^{b} ± 0.003
	30	0.3	15	*6.0*	0.0	0.373^{a} ± 0.014	0.433^{d} ± 0.005	0.140^{cd} ± 0.005	0.021^{c} ± 0.003
	30	0.3	15	*6.6*	0.0	0.363^{a} ± 0.035	0.417^{c} ± 0.007	0.129^{bc} ± 0.007	0.020^{c} ± 0.002
	30	0.3	15	*6.9*	0.0	0.331^{a} ± 0.020	0.376^{b} ± 0.008	0.119^{b} ± 0.008	0.026^{c} ± 0.003
	30	0.3	15	*7.6*	0.0	0.316^{a}± 0.040	0.347^{a} ± 0.009	0.089^{a} ± 0.007	0.006^{a} ± 0.001
NaCl	50	1.0	57	6.6	*0.00*	0.951^{a} ± 0.112	1.357^{a} ± 0.198	0.299^{a} ± 0.069	0.038^{a} ± 0.004
	50	1.0	57	6.6	*0.03*	1.265^{b} ± 0.086	1.951^{b} ± 0.189	0.351^{ab} ± 0.050	0.043^{ab} ± 0.004
	50	1.0	57	6.6	*0.06*	1.477^{b} ± 0.161	2.577^{c} ± 0.290	0.422^{bc} ± 0.057	0.049^{bc} ± 0.004
	50	1.0	57	6.6	*0.12*	1.821^{c} ± 0.101	3.804^{d} ± 0.214	0.521^{c} ± 0.068	0.053^{c} ± 0.002

* 'R_0', initial hydraulic resistance; 'R_∞', infinite (steady-state) hydraulic resistance; 'R_E', resistance increment extent and 'k' resistance increment rate.

Table 3
Effect of increasing temperature, pH, TMP, flow rate, and NaCl concentration on changes (%) of the exponential kinetic model parameters*

Parameters	Range	R_0 (1/m)	R_∞ (1/m)	R_E	K (1/s)
TMP (atm)	0.30 - 0.60	0.50	0.56	4.21	3.81
	0.60 – 1.00	0.71	0.42	2.78	6.21
T (°C)	30 - 40	-7.85	11.59	6.78	29.54
	40 - 50	-3.09	5.05	3.01	18.75
FR (L/min)	10 - 30	-0.31	-0.77	-0.83	-2.14
	30 - 46	-0.41	-0.62	-0.61	-2.08
pH	5.60 – 6.00	-4.64	-4.73	-0.51	6.53
	6.00 - 6.60	-0.45	-0.62	-1.31	-0.86
	6.60 - 6.90	-2.94	-3.28	-2.58	5.21
	6.90 - 7.60	-0.50	-0.77	-2.41	-6.45
NaCl (%)	0.00 - 0.03	11.01	14.59	5.80	4.39
	0.03 - 0.06	5.59	10.70	6.74	4.65
	0.06 - 0.12	5.01	8.37	5.88	1.36

* 'R_0', initial hydraulic resistance; 'R_∞', infinite (steady-state) hydraulic resistance; 'R_E', resistance increment extent and 'k' resistance increment rate.

Also, there is always an aggregation of particles close to the membrane surface which can act as a filter cake. As this cake develops, the hydraulic resistance increases [25]. Higher TMP may consequence in a higher deformation of the molecules and a higher cake compression [17, 26]. Also, the membrane resistance for polymeric membranes increases with increasing TMP and operating time due to membrane compaction [27]. Bahnasawy and Shenana [28] found that the medium resistance increased linearly with the time at different operational pressures, with greater increase at higher TMP, during the concentrating of milk. Grandinson et al. [27] found that both reversible and irreversible fouling increased with increasing TMP during ultrafiltration of skim milk. With decrease in TMP, membrane fouling would be alleviated, but permeate flux and filtration efficiency would drop [29]. Selecting a suitable TMP could improve permeate flux and control membrane fouling.

4.4. Effect of crossflow velocity

Results showed that during all the trials the Reynolds number (*Re*) inside the module was in the range of 383.73-2651.12. The laminar regime was obtained in most runs (*Re* < 2100) which is a typical regime in the hollow fiber modulus [30], except of those at FR higher than 30 L/min which showed transient regime (2100 < *Re* < 4000). As FR increased from 10 to 46 L/min, the *Re* increased from 465.11 to 2139.50 and transformed from laminar to transient regime (ρ_{ave} = 998.2 kg.m^{-3} and μ_{ave} = 646×10^{-6} Pa.s at 50 °C). Table 2 presents the hydraulic resistance modeling results under various UF crossflow velocities. It can be seen that R_0, R_∞, R_E and *k* decreased as FR increased from 10 to 46 L/min. In addition, *k* was the most affected parameter by the cross flow velocity (see Table 3). All parameters showed almost the same sensitivity to FR at 10-30 and 30-46 L/min ranges. The cross flow velocity has a role in detaching of particles (e.g. casein micelles, whey proteins or insoluble matter) away from the membrane surface by erosion, increase in back diffusion and shear enhanced diffusion [31]. Grandinson et al. [27] also found that the increase of wall shear stress resulted in the reduction in both reversible and irreversible fouling. Jaffrin et al. [32] compared the effects of various hydrodynamic parameters such as transmembrane pressure, shear rate, fluid viscosity and solute concentration on the permeate flux and found that flux was mainly governed by the maximum shear rate during skim milk ultrafiltration because very high shear rate effectively reduced concentration polarization.

4.5. Effect of feed pH

The variations in the exponential kinetic model parameters and R_E with pH of the feed are presented in Tables 2 and 3. R_0, R_E and R_∞ decreased with increase in the pH from 5.6-7.9 (see Table 2). Except at the range of 6-6.6 pH, at other ranges of pH, *k* was the most affected parameter during UF process. The most effective range of pH on R_0, R_∞ and *k* was the lowest pH range (5.60-6.00), while it was at the range of 6.60-6.90 (2.58%) for R_E (see Table 3). Reduction of pH would decrease the surface charge of particles in skimmed milk, such as whey proteins and casein micelles; thereby, decreases the repulsive electrostatic forces both between proteins and between proteins and the membrane surface. Consequently, proteins tend to deposit more on the membrane surface which led to higher total hydraulic resistance.

Furthermore, ionic calcium concentration increases as pH decreases, so it may cause an increase in fouling [25]. Also, the effective radius of solute molecules may decrease at low pH, making it easier to be adsorbed onto membrane surface. On the other hand, under alkaline conditions, membrane charge and hydrophilicity are improved, so, electrostatic repulsion between membrane and solutes reduces the concentration polarization and membrane fouling [21]. This result is in agreement with those reported for BSA solution by Chen et al. [31]. Youravong, Grandison and Lewis [33] also observed irreversible fouling increased with the decrease of pH during ultrafiltration of skim milk.

4.6. Effect of feed ionic strength

The results of dynamic modeling of hydraulic resistance at four NaCl concentrations (0, 0.03, 0.06 and 0.12 %w/w) are revealed in Table 2. According to this table, R_0, R_∞, R_E and *k* increased as NaCl concentration increased from 0 to 0.12 %w/w. The most important range of NaCl concentration on R_0 and R_∞ was the lowest range (0-0.03%), while it was 0.03-0.06% for other two parameters (see Table 3). R_∞ was the most affected parameter by NaCl concentration at all concentration ranges. Ionic strength impacts on the interaction within the cake layer and the porosity or packing density of the deposition. When NaCl is added to skim milk, due to a decrease in electrostatic repulsion force, a tighter fouling layer forms and causes pore blocking and formation of a more compact cake layer [21]. Furthermore, increasing ionic strength leads to an increase in ionic calcium. The calcium ions of milk are assumed to form bonds in the deposit between the membrane and the micelles and between micelles themselves [3, 34]. Youravong et al. [33] reported irreversible fouling increased with increase in the ionic strength of skim milk during ultrafiltration. Babu and Gaikar [35] also found that the protein layer resistance increased with an increase in salt concentration.

4.7. Sensitivity analysis

Sensitivity analysis (SA) has been used to study the uncertainty of the output relative to the uncertainty of different inputs to identify the relevant input factors [36]. Among several methods of SA (e.g., scatter plot, ANOVA and variance-based), regression analysis method was conducted in this study. Regression analysis, in the context of sensitivity analysis, contains fitting a linear regression to the model response and uses standardized regression coefficients as direct measures of sensitivity. As given in Table 4, NaCl concentration was the most effective factor in predicting the total hydraulic resistance (R_T) in milk UF process, while flow rate had the lowest effect on it. In addition, sensitivity analysis of exponential kinetic model parameters revealed that NaCl concentration and FR showed the highest and lowest impact on both R_0 *and* R_∞ parameters, respectively. R_E was mainly affected by temperature, while FR almost did not show significant effect on R_E. Among other input variables, TMP showed the highest impact on *k*, while similar to other parameters, FR showed the least impact on *k*.

Table 4
Sensitivity analyses of the input parameters for prediction of dynamic hydraulic resistance and exponential kinetic model parameters in crossflow ultrafiltration of skim milk.

Parameters	R_t (1/m)	R_0 (1/m)	R_∞ (1/m)	R_E (1/m)	K (1/s)
TMP (1atm)	0.35	0.43	0.29	0.19	0.60
T (°C)	0.05	0.45	0.44	0.77	0.18
FR (L/min)	-0.01	-0.06	-0.04	-0.09	-0.16
pH	-0.12	-0.16	-0.19	-0.20	-0.11
NaCl (%)	0.70	0.48	0.68	0.35	0.44
Time (min)	0.19	-	-	-	-

5. Conclusions

In this research, three semi-empirical models applied to better understand the kinetic of hydraulic resistance pattern in ultrafiltration of skim milk, as a case study. All three mentioned models, which didn't used for description of the membrane hydraulic resistance kinetics so far, were greatly significant for modelling the dynamic hydraulic resistance of skim milk (R^2 =0.801-0.998 and RMSE =0.002-2.502), but from the point of being in better agreement with the experimental data, the exponential kinetic model did the best. From the results obtained in this paper, the effect of TMP, temperature, crossflow velocity, NaCl concentration, and pH played important roles in resistance-time pattern. Except to *k* parameter which increased as pH increased, with increasing the flow rate and pH all the hydraulic resistance parameters increased. With each 1°C temperature, 0.1 atm TMP, 1 L/min FR and 1 unit pH increase, the most affected exponential kinetic model parameter at all the corresponding ranges was *k*, while R_∞ was the most affected parameter with each 1% NaCl concentration enhancement. Furthermore, sensitivity analysis indicated that among the input variables, NaCl concentration was the most sensitive factor for prediction of R_T, R_0 *and* R_∞, while temperature and TMP showed the most impact on R_E and *k*, respectively.

References

[1] M. Cheryan, Ultrafiltration Handbook, Technomic Publishing Co., Lancaster, Basel, 1986.
[2] G. Brans, C.G.P.H. Schröen, R.G.M. van der Sman, R.M. Boom, Membrane fractionation of milk: state of the art and challenges, J. Membr. Sci. 243 (2004) 263–272.
[3] K. Dewettinck, T.T. Le, Membrane separations in food processing, in: A. Proctor (Eds.), Alternatives to conventional food processing. RSC Publishing, Cambridge, UK, 2011, pp. 184-253.
[4] J.L. Soler-Cabezas, M. Tora`-Grau, M.C. Vincent-Vela, J.A. Mendoza-Roca, F.J. Martı´nez Francisco, Ultrafiltration of municipal wastewater: study on fouling models and fouling mechanisms, Desalin. Water Treat. 56 (2015) 3, 3427-34.
[5] V.S. Mamtani, K.P. Bhattacharyya, S. Prabhakar, P.K. Tewari, Fouling studies of capillary ultrafiltration membrane, Desalin. Water Treat. 52 (2014) 542-551.

[6] K.L. Jones, C.R. O'Melia, Protein and humic acid adsorption onto hydrophilic membrane surfaces: effects of pH and ionic strength, J. Membr. Sci. 165 (2000) 31-46.
[7] A. Alghooneh, S.M.A. Razavi, S.M. Mousavi, Nanofiltration treatment of tomato paste processing wastewater: process modeling and optimization using response surface methodology, Desalin. Water Treat. 57 (2016) 9609-9621.
[8] C.Y. Ng, A.W. Mohammad, L.W. Ng, J.M.D. Jahim, Membrane fouling mechanisms during ultrafiltration of skimmed coconut milk, J. Food Eng. 142 (2014) 190-200.
[9] P. Rai, G.C. Majumdar, S. Dasgupta, S. De, Modeling the performance of batch ultrafiltration of synthetic fruit juice and mosambi juice using artificial neural network, J. Food Eng. 71 (2005) 273–281.
[10] C. Bhattacharjee, S. Datta, Analysis of polarized layer resistance during ultrafiltration of PEG-6000: an approach based on filtration theory, Sep. Purif. Technol. 33 (2003) 115-126.
[11] S.M.A. Razavi, S.A. Mortazavi, S.M. Mousavi, Dynamic modeling of milk ultrafiltration by artificial neural network, J. Membr. Sci. 220 (2003) 47-58.
[12] S.M.A. Razavi, S.M. Mousavi, S.A. Mortazavi, Dynamic prediction of milk ultrafiltration performance: A neural network approach, Chem. Eng. Sci. 58 (2003) 4185-4195.
[13] S.M.A. Razavi, S.M. Mousavi, S.A. Mortazavi, Application of neural networks for crossflow milk ultrafiltration simulation, Int. Dairy J. 14 (2004) 69-80.
[14] J. Malave-Lopez, M. Peleg, Linearization of the electrostatic charging and charge decay curves of powders, Powder Technol. 42 (1985) 217–223.
[15] M. Peleg, An empirical model for the description of moisture sorption curves, J. Food Sci. (1988) 1216-1219.
[16] M. Peleg, Linearization of relaxation and creep curves of solid biological materials, J. Rheol. 24 (1980) 451-463.
[17] K. Konieczny, Modelling of membrane filtration of natural water for potable purposes, Desalination 143 (2002) 123-139.
[18] M. Rajca, M. Bodzek, K. Konieczny, Application of mathematical models to the calculation of ultrafiltration flux in water treatment, Desalination 239 (2009) 100-110.
[19] S.G. Yiantsios, A.J. Karabelas, The effect of colloid stability on membrane fouling, Desalination 118 (1998) 143-152.
[20] K.F. Eckner, E.A. Zottola, Modeling flux of skim milk as a function of pH, acidulant and temperature, J. Dairy Sci. 75 (1992) 2952-2958.
[21] W. Zhang, J. Luo, L. Ding, M.Y. Jaffrin, A review on flux decline control strategies in pressure-driven membrane processes, Ind. Eng. Chem. Res. 54 (2015) 2843-2861.
[22] A. Salahi, M. Abbasi, T. Mohammadi, Permeate flux decline during UF of oily wastewater: experimental and modeling, Desalination 251 (2010) 153-160.
[23] P. Bacchin, P. Aimar, R. Field, Critical and sustainable fluxes: theory, experiments and applications, J. Membr. Sci. 281 (2006) 42-69.
[24] C.L. Astudillo-Castro, Limiting flux and critical transmembrane pressure determination using an exponential model: the effect of concentration factor, temperature, and cross-flow velocity during casein micelle concentration by microfiltration, Ind. Eng. Chem. Res. 54 (2015) 414-425.
[25] P. Bacchin, P. Aimar, V. Sanchez, Model for colloidal fouling of membranes, AIChE. J. 41 (1995) 368-376.
[26] P. Bacchin, D. Si-Hassen, V. Starov, M.J. Clifton, P. Aimar, A unifying model for concentration polarization, gel-layer formation and particle deposition in crossflow membrane filtration of colloidal suspensions, Chem. Eng. Sci. 57 (2002) 77-91.
[27] A. Grandison, W. Youravong, M.J. Lewis, Hydrodynamic factors affecting flux and fouling during ultrafiltration of skimmed milk, Lait 80 (2000) 165-174.
[28] A.H. Bahnasawy, M.E. Shenana, Flux behavior and energy consumption of ultrafiltration (UF) process of milk, Australian J. Agr. Eng. 1 (2010) 54-65.
[29] W. Zhang, Z. Zhu, M. Y. Jaffrin, L. Ding, Effects of hydraulic conditions on effluent quality, flux behavior, and energy consumption in a shear-enhanced membrane filtration using Box-Behnken response surface methodology, Ind. Eng. Chem. Res. 53 (2014) 7176-7185.
[30] A.L. Zydney, Module design and membrane configurations, in: L.J. Zeman (Eds.), Microfiltration and Ultrafiltration: Principles and Applications, CRC Press, New York, 1996, PP. 333.
[31] V. Chen, A.G. Fane, S. Madaeni, I.G. Wenten, Particle deposition during membrane filtration of colloids: transition between concentration polarization and cake formation, J. Membr. Sci. 125 (1997) 109-122.
[32] M.Y. Jaffrin, L-H. Ding, O. Akoum, A. Brou, A hydrodynamic comparison between rotating disk and vibratory dynamic filtration systems, J. Membr. Sci. 242 (2004) 155-167.
[33] W. Youravong, A.S. Grandison, M.J. Lewis, The effect of physico-chemical changes on critical flux of skimmed milk ultrafiltration, SJST. 24 (2002) 929-939.
[34] M. Rabiller-Baudry, H. Bouzid, B. Chaufer, L. Paugam, D. Delaunay, O. Mekmene, S. Ahmad, F. Gaucheron, On the origin of flux dependence in pH modified skim milk filtration, Dairy Sci. Technol. 89 (2009) 363-385.
[35] P.R. Babu, V.G. Gaikar, Membrane characteristics as determinant in fouling of UF membranes, Sep. Purif. Technol. 24 (2001) 23-34.
[36] A. Saltelli, A. Tarantola, F. Campolongo, M. Ratto, Sensitivity analysis in practice, Wiley, New York, 2004.